



## Article

# Influence of Tungsten Nanoparticles on Microstructure and Mechanical Properties of an Al-5%Mg Alloy Produced by Casting

Anton Khrustalyov \* , Nikolay Kakhidze , Vladimir Platov, Ilya Zhukov  and Alexander Vorozhtsov

Faculty of Physics and Engineering, National Research Tomsk State University, 634050 Tomsk, Russia; nick200069@yandex.ru (N.K.); vova.platov.85@mail.ru (V.P.); gofra930@gmail.com (I.Z.); abv1953@mail.ru (A.V.)

\* Correspondence: tofik0014@gmail.com; Tel.: +7-952-1555-568

**Abstract:** This paper investigates the impact of tungsten nanoparticles on the microstructure and mechanical properties of the Al-5Mg alloy. Tungsten concentrations of up to 0.5 wt.% led to a slight modification of the Al-5Mg alloy microstructure, and grain refinement occurred due to the inhibition of crystal growth along the boundaries. Dispersion hardening with tungsten nanoparticles made it possible to increase the ultimate strength by the Orowan mechanism with a simultaneous increase in the plasticity of the Al-5Mg alloy. An increase in the tungsten content to 0.8 wt.% made it possible to modify the microstructure of the Al-5Mg alloy, due to the formation of the Al<sub>12</sub>W phase and an increase in crystallisation centres. The modification of the microstructure, as well as dispersion strengthening by nanoparticles, led to a simultaneous increase in the yield strength, ultimate tensile strength, and ductility of the Al-5Mg alloy.



**Citation:** Khrustalyov, A.; Kakhidze, N.; Platov, V.; Zhukov, I.; Vorozhtsov, A. Influence of Tungsten Nanoparticles on Microstructure and Mechanical Properties of an Al-5%Mg Alloy Produced by Casting. *Metals* **2022**, *12*, 989. <https://doi.org/10.3390/met12060989>

Academic Editors: Francesco Iacoviello and Angelo Fernando Padilha

Received: 12 April 2022

Accepted: 26 May 2022

Published: 9 June 2022

**Publisher's Note:** MDPI stays neutral with regard to jurisdictional claims in published maps and institutional affiliations.



**Copyright:** © 2022 by the authors. Licensee MDPI, Basel, Switzerland. This article is an open access article distributed under the terms and conditions of the Creative Commons Attribution (CC BY) license (<https://creativecommons.org/licenses/by/4.0/>).

**Keywords:** metal matrix composites; nanoparticles; tungsten; microstructure; mechanical properties; fracture

## 1. Introduction

Aluminium-based metal matrix composites (MMCs) are attractive to the automotive, marine, aerospace, etc., industries due to a combination of their physical and mechanical properties and oxidation resistance [1,2]. Non-metallic powders (oxides, carbides, intermetallics, etc.) are widely used as reinforcing particles in aluminium MMCs. These reinforcing particles are introduced by the ex situ [3] method, where reinforcing particles are synthesised before being introduced into the matrix, or by the in situ [4–6] method, where initial materials are introduced into the metal matrix for the reaction to synthesise reinforcing fibre particles. When using the ex situ method, it is possible to set the dispersion and phase composition parameters for the reinforcing particles in advance; for dispersion strengthening, Al<sub>2</sub>O<sub>3</sub> [7,8], SiC [9,10], B<sub>4</sub>C [11,12], etc., particles are commonly applied. The most effective strengthening is achieved with the use of nanoparticles to obtain metal matrix nanocomposites (MMNCs), but this requires their uniform distribution within the metal matrix volume. In [13], an Al/Al<sub>3</sub>Ti composite was obtained, the Young's modulus of which amounted to 110 GPa, 57% more than the initial alloy. In this case, the nanoparticles must be evenly distributed within the volume of the aluminium matrix and provide a strong bond with it, which should be retained during the dislocation motion. Producing MMCs and MMNCs is possible using a variety of methods, but casting technology is the most versatile [14,15]. Meanwhile, fabricating MMCs by casting is associated with a number of problems, including the agglomeration of nanoparticles and the flotation of particles on the melt surface due to their poor wettability [16–19]. As a result, there is a decrease in the composite density and heterogeneity of its structure, leading to a decrease in its mechanical properties. The solution to this problem is possible in several ways, namely, by

forming coatings on the particles to increase their wettability [20], by using master alloys, and by applying external fields (ultrasonic, mechanical treatment) to the melt.

The Al-5%Mg alloy is mainly used in the form of sheets after deformation and heat treatment. The highest properties of this alloy are achieved due to dispersion strengthening, by introducing such elements as Sc and Zr [21–23]. The main disadvantage of using scandium and zirconium is their high cost, resulting in a significant increase in material cost. A number of papers report on using tungsten to produce aluminium-based MMCs. The casting process makes it possible to provide an interaction [24–27] of metallic tungsten with an aluminium matrix and form such intermetallic compounds as  $Al_4W$ ,  $Al_5W$ , and  $Al_{12}W$ ; the process will combine in situ and ex situ methods within the same technology [28].

In this study, the research team used tungsten nanoparticles to fabricate aluminium MMCs. In connection to the aforementioned, it is known that tungsten has a high melting point, strength, and a low coefficient of thermal expansion (CTE). Studies on such materials have shown a significant increase in the mechanical and functional properties of aluminium alloys [29]. Tungsten particles and W-Al intermetallic compounds in the aluminium alloy can improve mechanical properties, such as strength, hardness, oxidation resistance, and thermal stability compared to the initial Al and W. The low solubility of W in aluminium alloys and its reactivity makes it possible to obtain an aluminium MMC reinforced with nanoparticles, which are distributed in the metal matrix.

Thus, the aim of this study was to explore the impact of the content of tungsten nanoparticles on the microstructure and mechanical properties of the Al-Mg alloy after casting.

## 2. Materials and Research Methods

### 2.1. Obtaining the Composites

The Al-5Mg (Al—95 wt.%, Mg—5 wt.%) alloy was used as an initial alloy. Tungsten powder, obtained by the electrical explosion of a conductor, was used as strengthening particles. Figure 1 shows the scanning electron microscopy (SEM) (Figure 1a) and the transmission electron microscopy (TEM) (Figure 1b) images of W nanoparticles.

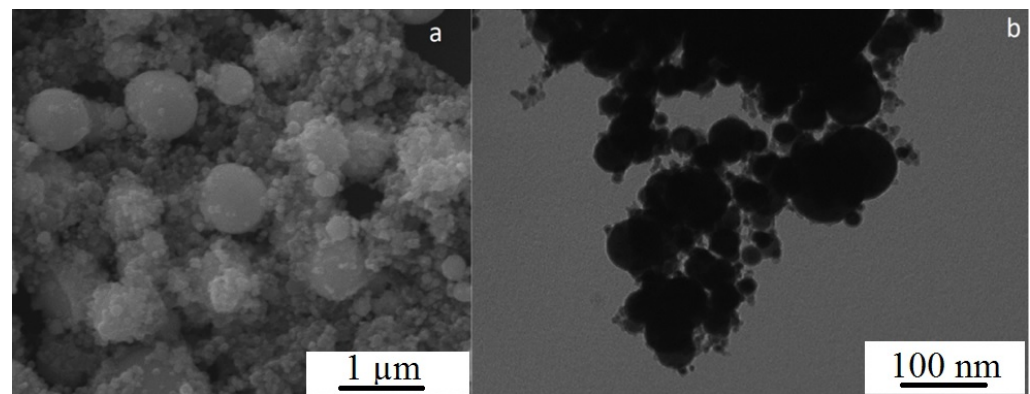


**Figure 1.** Images of W nanoparticles: (a) SEM; (b) TEM.

W powder particles have a regular spherical shape (Figure 1), formed during the electrical explosion of the conductor. The average size of a W particle is 200 nm (Figure 1b). In the W powder, large metallic particles are observed, the size of which reaches 10 μm.

One thousand grams of the Al-5Mg alloy was placed into a graphite crucible, melted in a muffle furnace at a temperature of 780 °C, and aged for 2 h. The crucible was then removed from the furnace with a gripper, and the master alloy Al-W was introduced while being subjected to ultrasonic treatment melt at a temperature of 730 °C. Tungsten particles were introduced in Al—5wt.% W master alloy, which was obtained by mixing in a planetary mill and pressing on a hydraulic press at a load of 0.5 tons. The ultrasonic treatment melt was performed using a magnetostrictive water-cooled transducer PMS-5-8 ( $W = 4.1$  kV,  $f = 17.6$  kHz, RELTEC, Ekaterinburg, Russia). After complete dissolution of the master alloy

(absence of undissolved master alloy and its parts in the melt), the ultrasonic treatment was performed for 2 min. At a temperature of 720 °C, the melt was poured into a coquille. The amount of W nanoparticles in the alloy varied from 0 to 0.8 wt.%. The Al-5Mg initial alloy was obtained under similar casting parameters without introducing W nanoparticles. The obtained alloy samples were flat castings 10 mm thick, 100 mm wide, and 150 mm high.

## 2.2. Research Methodology for Studying Initial Materials and Composites

The structure of the W nanoparticles was studied by TEM using a JEOL JEM-2100 microscope (JEOL Ltd., Akishima, Japan). Research alloys were used in their initial cast form without heat and mechanical treatment to assess the effect of “ex situ” W nanoparticles on the dispersion strengthening of the Al-5Mg alloy. The microstructures of the obtained materials were investigated through SEM using a Quanta 200 3D (FEI Company, Hillsboro, OR, USA) microscope, and optical microscopy using an Olympus GX71 microscope (Olympus, Tokyo, Japan). The particle dispersion was analysed using the images obtained by the secant method. Phase analysis of the alloys was performed using a Shimadzu XRD 6000 X-ray diffractometer (Shimadzu, Tsukinowa, Japan) with filtered CuK $\alpha$  radiation at diffraction angles from 20° to 80° with 0.1° step and an exposure time of 10 s. Mechanical tests were performed using a universal testing machine, Instron 3369 (Instron European Headquarters, High Wycombe, UK), at a gripping speed of 0.2 mm/min. The specimens were cut from the castings using electroerosive cutting and were in the form of flat blades, 2 mm thick with a ratio of the width of the working part to the gripping point  $\geq 1.5$ . The tests were carried out according to ASTM B557-15. The samples for research were cut from the upper, middle, and lower parts (relative height) of the casting.

## 3. Results and Discussion

Figure 2 presents optical images of the microstructure of the aluminium alloys.

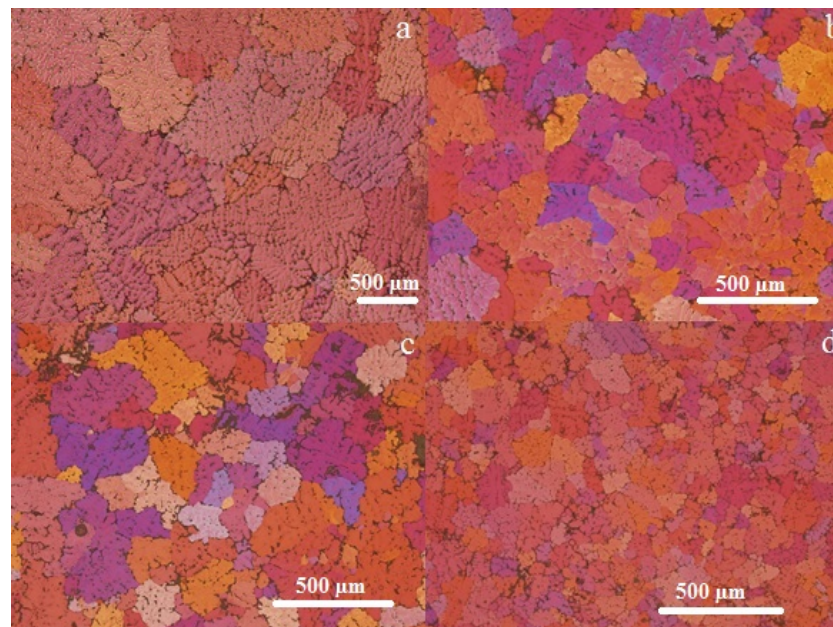


**Figure 2.** Optical images of the microstructure of the Al-5Mg (a), Al-5Mg-0.3W (b), Al-5Mg-0.5W (c), and Al-5Mg-0.8W (d) alloys.

The microstructure of the initial Al-5Mg alloy is made up of equiaxed grains with an average size of 180  $\mu\text{m}$ . The introduction of 0.3 and 0.5 wt.% W does not lead to a significant decrease in the average grain size, which was 164 and 149  $\mu\text{m}$ , respectively. However, an increase in the content of W nanoparticles in the Al-5Mg alloy to 0.8 wt.% leads to a decrease in the average grain size to 95  $\mu\text{m}$ . It is known that grain refinement in

aluminium alloys is possible due to the nucleation and inhibition of grain growth during melt solidification [30]. The formation of new solidification centres requires the formation of a phase with a coherent structure, on which further grain growth is possible. For the Al-W system, the  $Al_{12}W$  intermetallide can act as a solidification centre, but according to the data of X-ray diffraction (XRD) analysis (Figure 3), this phase cannot be identified.

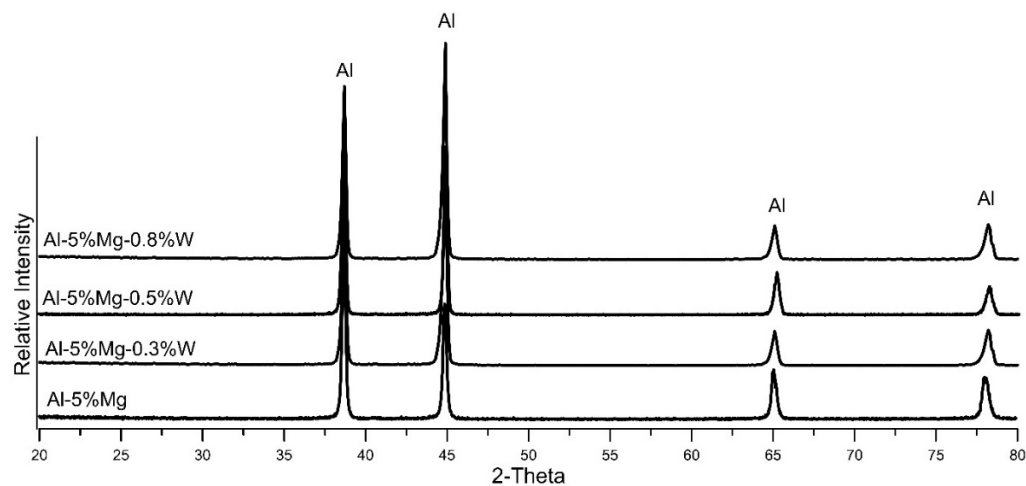


**Figure 3.** Results of XRD analysis of Al-5Mg alloys.

In addition, in the case of the formation of  $Al_{12}W$ , which occurs at a concentration of more than 0.3 wt.% W in aluminium [31], grain refinement could also be observed in alloys Al-5Mg-0.3W and Al-5Mg-0.5W.

In the microstructure of the Al-5Mg alloy, there are inclusions of pores with a size of no more than  $\sim 1 \mu m$  (Figure 4a). At the same time, the alloy microstructure is quite uniform, without a visible accumulation of pores. The introduction of 0.3 wt.% W did not lead to a significant change in the microstructure compared to the initial alloy, and no accumulation of nanoparticle agglomerates was observed in the microstructure (Figure 4b). A deeper analysis of the microstructure makes it possible to reveal individual particles of tungsten in the Al-5Mg-0.3W alloy, which are displaced into pores due to the movement of the solidification front during the cooling of the melt (Figure 5a, Table 1). An increase in the W content to 0.5 wt.% does not lead to a change in the microstructure of the alloy at magnifications of up to  $\times 1000$  (Figure 4c). However, at high magnifications, both individual W particles and their agglomerates can be observed, which are located in the volume of grains and interboundary regions (Figure 5c, Table 1).

**Table 1.** Results of EDS analysis of Al-5Mg alloys (see Figure 5).

Point Number	Al, wt%	W, wt.%	Mg, wt%	O, wt%
1	87.75	-	3.07	9.18
2	81.92	-	4.73	13.35
3	93.69	-	2.09	4.22
4	-	100	-	-
5	19.62	80.38	-	-
6	0.79	99.21	-	-
7	80.16	19.84	-	-
8	56.78	43.22	-	-



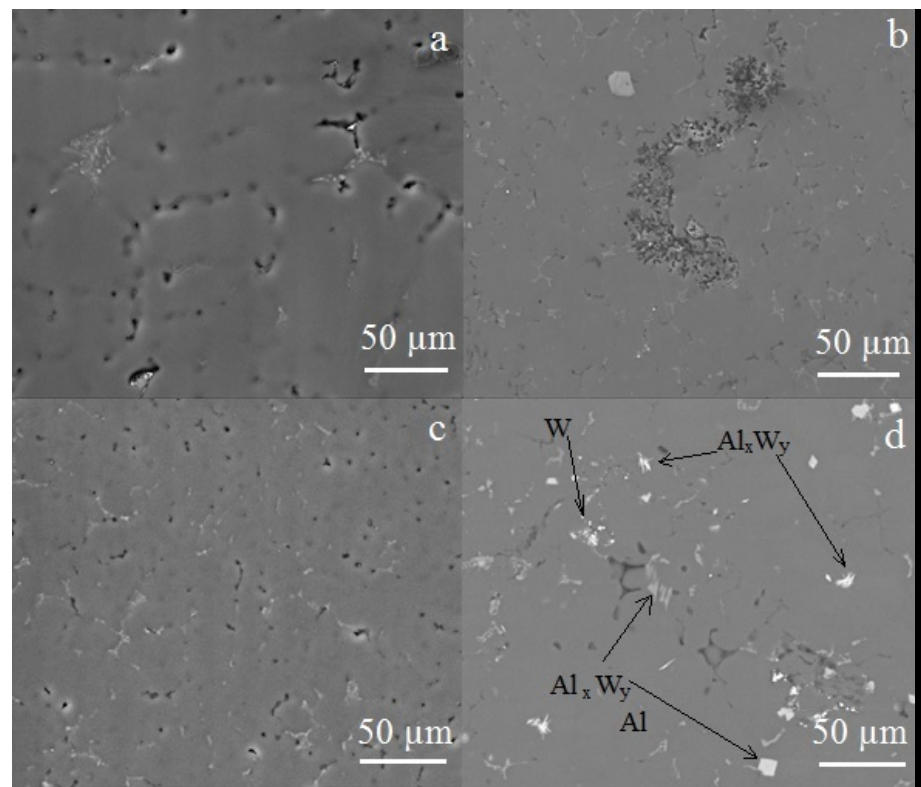


**Figure 4.** The SEM image of Al-Mg alloys: (a) Al-5Mg, (b) Al-5Mg-0.3W, (c) Al-5Mg-0.5W, and (d) Al-5Mg-0.8W.

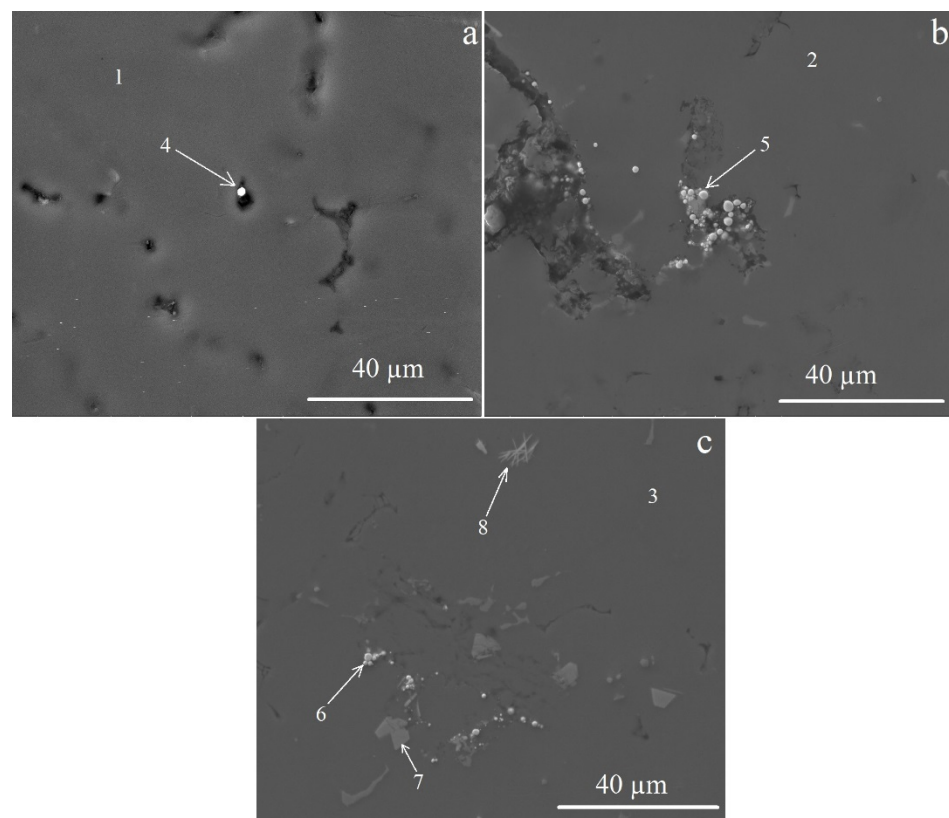


**Figure 5.** The SEM image of Al-Mg-W alloys: (a) Al-5Mg-0.3W, (b) Al-5Mg-0.5W, (c) Al-5Mg-0.8W.

An increase in the W content to 0.8 wt.% led to a significant increase in nanoparticles and their agglomerates in the volume and at grain boundaries (Figure 4d). In addition, the microstructure of the Al-5Mg-0.5W alloy contains irregularly shaped particles up to 10  $\mu\text{m}$  in size, as well as inclusions in the form of a “needle” with a thickness of less than 500 nm and a length of up to 10  $\mu\text{m}$  (Figures 4d and 5c). According to the energy-dispersive X-ray spectroscopy (EDS) analysis data (Table 1), these phases contain aluminium and tungsten (points 7, 8), which indicates the formation of intermetallic compounds when 0.8 wt.% W is introduced into the melt, but their low content does not allow for their identification in XRD analysis (Figure 3). Irregularly shaped particles can be  $\text{Al}_4\text{W}$  or  $\text{Al}_{12}\text{W}$  intermetallic compounds [32], but the  $\text{Al}_4\text{W}$  phase is formed in liquid aluminium at temperatures above 700 °C and is retained only under conditions of rapid cooling during solidification [33]. Acicular-shaped intermetallic inclusions are  $\text{Al}_5\text{W}$  (point 8), the particle shape of which differs significantly from  $\text{Al}_4\text{W}$  and  $\text{Al}_{12}\text{W}$  [33]. The formation of the  $\text{Al}_{12}\text{W}$  phase during solidification led to a refinement of the microstructure of the aluminium alloy (Figure 2d). Thus, the main mechanism of microstructure refinement at a content of W nanoparticles up to 0.5 wt.% in the Al-5Mg alloy is the inhibition of crystal growth along the boundaries, and at a content of more than 0.5 wt.%, the dominant mechanism is an increase in the number of solidification centres during melt cooling.

It can be seen from the stress–strain curves for the alloys obtained (Figure 6, Table 2) that the introduction of tungsten nanoparticles into the alloy leads to a simultaneous increase in the Al-5Mg alloy yield strength and ductility.

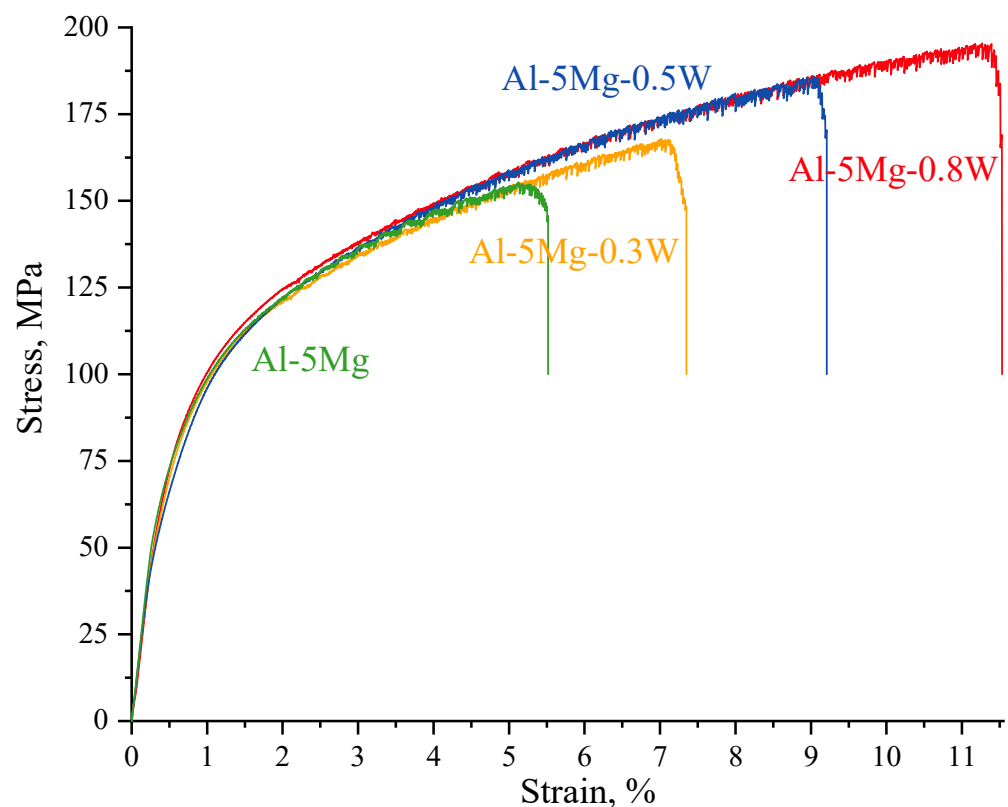


**Figure 6.** The stress–strain curves for the Al-5Mg and Al-5Mg-W alloys.

Introducing 0.3 wt.% of W nanoparticles results in an increase in the hardness from 57 to 64 HB, microhardness from 68 to 71 HV, yield strength from 80 to 85 MPa, and ductility from 5.2 to 6.4%. There is also a slight increase in the ultimate tensile strength from 155 to 164 MPa. The introduction of 0.5 wt.% W nanoparticles led to an increase in hardness from 64 to 69 HB, ultimate tensile strength from 164 to 185 MPa, and ductility from 6.4 to 8.5%. At the same time, there is no increase in microhardness and yield

strength, which amounted to 73 HV and 79 MPa, respectively (Table 2). An increase in the content of W nanoparticles to 0.8 wt.% made it possible to increase the hardness from 69 to 75 HB, the microhardness from 73 to 81 HV, the yield strength from 79 to 91 MPa, the ultimate tensile strength from 185 to 194 MPa, and the ductility from 8.5 to 10.3%. Based on the microstructure (Figures 2, 4 and 5), it can be assumed that the increase in mechanical properties (yield strength and ultimate tensile strength) Al-5Mg aluminium alloy is due to the Hall–Petch law, Orowan mechanisms [1,34], the difference in the (CTEs) for the matrix and particles [35], and the load transfer from particles to the matrix [36].

**Table 2.** Grain size, hardness, and tensile properties ( $\sigma_{0.2}$ —yield strength,  $\sigma_B$ —ultimate tensile strength,  $\epsilon_{\max}$ —ductility) of the aluminium alloys obtained.

Alloy	Grain Size, $\mu\text{m}$	Hardness, HB	Microhardness, HV	$\sigma_{0.2}$ , MPa	$\sigma_B$ , MPa	$\epsilon_{\max}$ , %
Al-5Mg	180 $\pm$ 5	57 $\pm$ 3	68 $\pm$ 9	80 $\pm$ 2	155 $\pm$ 6	5.2 $\pm$ 0.4
Al-5Mg-0.3W	164 $\pm$ 4	64 $\pm$ 1.2	71 $\pm$ 10	85 $\pm$ 1.6	164 $\pm$ 5	6.4 $\pm$ 0.7
Al-5Mg-0.5W	149 $\pm$ 6	69 $\pm$ 1	73 $\pm$ 9	79 $\pm$ 1	185 $\pm$ 7	8.5 $\pm$ 0.5
Al-5Mg-0.8W	95 $\pm$ 4	75 $\pm$ 2	81 $\pm$ 7	91 $\pm$ 2.2	194 $\pm$ 6	10.3 $\pm$ 0.7

The contribution of grain refinement to the improvement of the yield strength of the Al-5Mg aluminium alloy can be calculated by the Hall–Petch relationship [23]:

$$\sigma_{GR} = k_y \left( D^{-\frac{1}{2}} - D_0^{-\frac{1}{2}} \right), \quad (1)$$

where  $D$ —modified alloy grain size,  $D_0$ —grain size of the initial alloy, and  $k_y$ —Hall–Petch coefficient (68 MPa). The contribution of the Hall–Petch law for Al-5Mg alloy upon introduction of 0.3, 0.5 and 0.8 wt.% W enhances the mechanical properties of Al-5Mg alloy by 1.6, 1.7 and 6.9 MPa, respectively. Thus, the Hall–Petch law contributes to an increase in the yield strength of the Al-5Mg-0.8W alloy due to the refinement of the microstructure of the aluminium matrix in the process of modification with the  $\text{Al}_{12}\text{W}$  intermetallic compound.

The contribution of the load transfer mechanism from the hardening particles to the metal matrix is calculated by the formula:

$$\sigma_{load} = 0.5V_p\sigma_{0.2}, \quad (2)$$

where  $V_p$  is the volume content of tungsten nanoparticles and  $\sigma_{0.2}$  is the yield strength of the matrix (80 MPa).

The contribution of the load transfer from the particles to the matrix [36] in this case was 0.58 MPa (Al-5Mg-0.3W), 0.92 MPa (Al-5Mg-0.5W), and 1.47 MPa (Al-5Mg-0.8W). This is due to the high density of W (19.25 g/cm<sup>3</sup>); the volume content of nanoparticles in the Al-5Mg alloy does not exceed ~0.08 vol.%.

The contribution of the Orowan mechanism [1] to the increase in the mechanical properties of the alloy was calculated by the formula:

$$\sigma_{OR} = \frac{0.13bG_m}{\lambda} \ln \frac{d_p}{2b} \quad (3)$$

where  $b$ —Burgers vector,  $G_m$ —shear modulus,  $d_p$ —diameter of particles, and  $\lambda$  the value taking into account the size and volume content of the particles, which is calculated by the formula:

$$\lambda = d_p \left( \left( \frac{1}{2V_p} \right)^{\frac{1}{3}} - 1 \right) \quad (4)$$

The calculated contribution of W nanoparticles to the mechanical properties of the Al-5Mg aluminum alloy by the Orowan mechanism was 22.2 MPa (Al-5Mg-0.3W), 30.5 MPa (Al-5Mg-0.5W), and 41 MPa (Al-5Mg-0.8W). The contribution of the difference between the matrix and particle CTEs [35] is calculated by the formula:

$$\Delta\sigma_{CTE} = \beta G b \left( \frac{12(\alpha_m - \alpha_p) \Delta T V_p}{b l_p (1 - V_p)} \right)^{\frac{1}{2}} \quad (5)$$

where  $l_p$ —the distance between the particles,  $\beta$ —constant (1.25),  $\alpha_m$ —metal matrix CTE ( $23 \times 10^{-6}$  1/K),  $\alpha_p$ —CTEs of the particles,  $\Delta T$ —the difference between the synthesis temperature (725 °C) and the room temperature (25 °C). The contribution of the mechanism of the difference between the CTE of the matrix and particles was less than 0.5 MPa for all obtained alloys. Thus, the dominant mechanism for increasing mechanical properties is the Orowan mechanism, due to dispersion strengthening by W nanoparticles. It should be noted that for the Al-5Mg-0.8W alloy, the deformation behaviour is more complex, due to the influence of W metal particles, Al<sub>12</sub>W intermetallic particles, and Al<sub>5</sub>W acicular inclusions, which contributes to a simultaneous increase in the ultimate tensile strength and ductility of the aluminium alloy.

The evaluation of the contribution of various mechanisms made it possible to identify the dominant mechanism for increasing the yield strength and ultimate tensile strength of the Al-5Mg alloy. However, at the same time, an increase in plasticity occurs with the introduction and increase in the content of tungsten nanoparticles. In [37], a similar relationship was observed for an aluminium alloy when the yield strength, ultimate tensile strength, and ductility increased. It is assumed that the introduction of particles into the grain body can result in a deviation of a potential crack from the grain boundary into its bulk, as well as in greater involvement of the metal matrix in the process of deformation and fracture [38,39]. Tungsten nanoparticles allow for a more efficient use of the aluminium matrix in the deformation process, similarly to non-metallic particles. In this case, it is metal tungsten nanoparticles that contribute to the plasticity of the aluminium matrix, which increases regardless of the formation of Al<sub>5</sub>W and Al<sub>12</sub>W intermetallic phases.

In general, the Al-5Mg alloy fracture (Figure 7a) is the pronounced one following the viscous transcrystalline mechanism. Introducing 0.3 wt.% W nanoparticles does not lead to a significant change in the fracture surface (Figure 7b). An increase in the content of nanoparticles leads to a mixed failure mechanism, due to the presence of nanoparticle agglomerates in the interboundary regions, which do not make it possible to achieve the maximum mechanical properties of the aluminium alloy (Figure 7c). The fracture of the Al-5Mg-0.8W alloy occurs according to the viscous transcrystalline mechanism (Figure 7d), due to the refinement of the alloy microstructure, which made it possible to avoid the brittle fracturing of the alloy along the grain boundaries that contain agglomerates of tungsten nanoparticles.



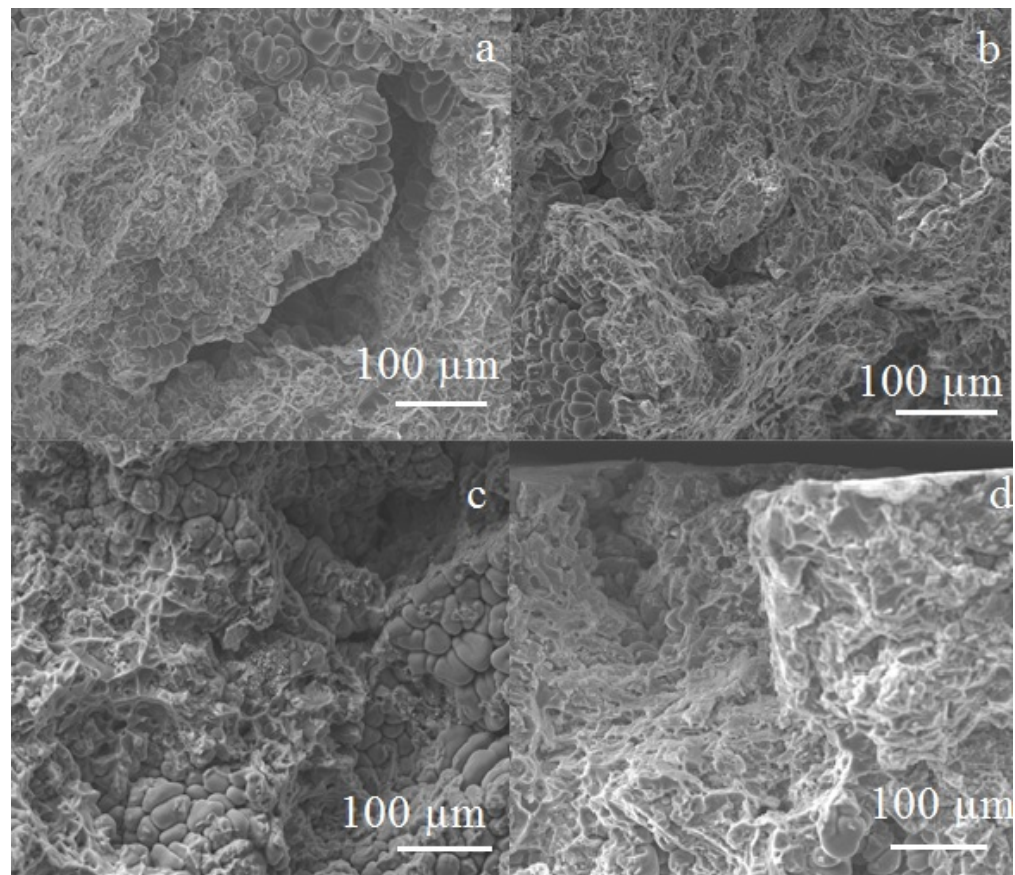


**Figure 7.** SEM images of the Al-Mg alloy fracture surface: (a) Al-5Mg, (b) Al-5Mg-0.3W, (c) Al-5Mg-0.5W, and (d) Al-5Mg-0.8W.

#### 4. Conclusions

It has been established that the introduction of 0.8 wt.% W nanoparticles makes it possible to reduce the average grain size of the Al-5Mg alloy from 180 to 95  $\mu\text{m}$  due to the formation of the  $\text{Al}_{12}\text{W}$  intermetallic phase. With the introduction of less than 0.8 wt.% of W nanoparticles in the Al-5Mg alloy, the average grain size decreases from 180 to 149  $\mu\text{m}$ , due to the inhibition of crystal growth during melt cooling.

The introduction of 0.8 wt.% W nanoparticles has increased the alloy hardness and microhardness from 57 to 75 HB and from 67 to 81 HV, respectively, the yield strength from 80 to 91 MPa, the ultimate tensile strength from 155 to 194 MPa, and the ductility from 5.2 to 10.3%. Using the data calculated, it has been shown that the dominant mechanisms for increasing the mechanical properties of the alloy are the Orowan mechanism and Hall–Petch law.

The introduction of up to 0.3 wt.% W nanoparticles does not lead to a significant change in the fracture surface of the alloy, but an increase to 0.5 wt.% leads to the implementation of a ductile–brittle mechanism. The refinement of the microstructure of the Al-5Mg alloy with the introduction of 0.8 wt.% W nanoparticles makes it possible to avoid brittle fractures along the grain boundaries that contain agglomerates of W nanoparticles.

**Author Contributions:** Conceptualization, A.K.; methodology, A.K. and I.Z.; formal analysis, N.K. and V.P.; investigation, V.P., N.K. and A.K.; supervision, A.V.; funding acquisition, A.K. All authors have read and agreed to the published version of the manuscript.

**Funding:** Obtaining master-alloys, aluminum alloys, as well as the study of the structure, phase composition, mechanical properties and fracture supported by Grant N 20-79-00060 from the Russian Science Foundation. The selection of melt processing parameters by external fields to obtain alloys

was supported by the Ministry of Education and Science of the Russian Federation (State assignment No. FSWM-2020-0028).

**Institutional Review Board Statement:** Not applicable.

**Informed Consent Statement:** Not applicable.

**Data Availability Statement:** The data presented in this study are available in the article.

**Acknowledgments:** The authors acknowledge Russian Science Foundation under Grant N 20-79-00060. The research was carried out with the equipment of Tomsk Regional Core Shared Research Facilities Center of National Research Tomsk State University (Grant of the Ministry of Science and Higher Education of the Russian Federation no. 075-15-2021-693 (no. 13.RFC.21.0012)).

**Conflicts of Interest:** The authors declare no conflict of interest.

## References

1. Samal, P.; Vundavilli, P.R.; Meher, A.; Mahapatra, M.M. Recent progress in aluminum metal matrix composites: A review on processing, mechanical and wear properties. *J. Manuf. Processes* **2020**, *59*, 131–152. [[CrossRef](#)]
2. Jones, R.H. The influence of hydrogen on the stress-corrosion cracking of low-strength Al-Mg alloys. *JOM* **2003**, *55*, 42–46. [[CrossRef](#)]
3. Kannan, C.; Ramanujam, R. Advanced liquid state processing techniques for ex-situ discontinuous particle reinforced 1216 nanocomposites: A review. *Sci. Technol. Mater.* **2018**, *30*, 109–119. [[CrossRef](#)]
4. Meti, V.K.V.; Shirur, S.; Nampoothiri, J.; Ravi, K.R.; Siddhalingeshwar, I.G. Synthesis, Characterization and Mechanical Properties of AA7075 Based MMCs Reinforced with TiB<sub>2</sub> Particles Processed Through Ultrasound Assisted In-Situ Casting Technique. *Trans. Indian Inst. Met.* **2018**, *71*, 841–848. [[CrossRef](#)]
5. Basak, A.K.; Pramanik, A.; Prakash, C. Deformation and strengthening of SiC reinforced Al-MMCs during in-situ micro-pillar 1051 compression. *Mater. Sci. Eng. A* **2019**, *763*, 138141. [[CrossRef](#)]
6. Chen, B.; Kondoh, K.; Li, J.S.; Qian, M. Extraordinary reinforcing effect of carbon nanotubes in aluminium matrix composites assisted by in-situ alumina nanoparticles. *Compos. Part B Eng.* **2020**, *183*, 107691. [[CrossRef](#)]
7. Ahamad, N.; Mohammad, A.; Gupta, P. Wear characteristics of Al matrix reinforced with Al<sub>2</sub>O<sub>3</sub>-carbon hybrid metal matrix composites. *Mater. Today Proc.* **2021**, *38*, 63–68. [[CrossRef](#)]
8. Yang, K.; Li, W.; Niu, P.; Yang, X.; Xu, Y. Cold sprayed AA2024/Al<sub>2</sub>O<sub>3</sub> metal matrix composites improved by friction stir processing: Microstructure characterization, mechanical performance and strengthening mechanisms. *J. Alloys Compd.* **2018**, *736*, 115–123. [[CrossRef](#)]
9. Adeosun, S.O.; Akpan, E.I.; Gbenebor, O.P.; Balogun, S.A. Ductility and hardness of chloride cleaned AA6011/SiCp composites. *Trans. Nonferrous Met. Soc. China* **2016**, *26*, 339–347. [[CrossRef](#)]
10. Goyal, H.; Mandal, N.; Roy, H.; Mitra, S.K.; Mondal, B. Multi Response Optimization for Processing Al-SiCp Composites: An Approach Towards Enhancement of Mechanical Properties. *Trans. Indian Inst. Met.* **2015**, *68*, 453–463. [[CrossRef](#)]
11. Abdizadeh, H.; Baghchesara, M.A. Optimized Parameters for Enhanced Properties in Al-B<sub>4</sub>C Composite. *Arab. J. Sci. Eng.* **2018**, *43*, 4475–4485. [[CrossRef](#)]
12. Khademian, M.; Alizadeh, A.; Abdollahi, A. Fabrication and Characterization of Hot Rolled and Hot Extruded Boron Carbide (B<sub>4</sub>C) Reinforced A356 Aluminum Alloy Matrix Composites Produced by Stir Casting Method. *Trans. Indian Inst. Met.* **2017**, *70*, 1635–1646. [[CrossRef](#)]
13. Sun, Z.; Hashimoto, H.; Wang, Q.; Park, Y.; Abe, T. Synthesis of Al-Al<sub>3</sub>Ti Composites using Pulse Discharge Sintering Process. *Mater. Trans.* **2000**, *41*, 597–600. [[CrossRef](#)]
14. Akbari, M.K.; Baharvandi, H.R.; Shirvanimoghaddam, K. Tensile and fracture behavior of nano/micro TiB<sub>2</sub> particle reinforced casting A356 aluminum alloy composites. *Mater. Des.* **2015**, *66*, 150–161. [[CrossRef](#)]
15. Katsarou, L.; Mounib, M.; Lefebvre, W.; Vorozhtsov, S.; Pavese, M.; Badini, C.; Molina-Aldareguia, J.M.; Jimenez, C.C.; Pérez Prado, M.T.; Dieringa, H. Microstructure, mechanical properties and creep of magnesium alloy Elektron21 reinforced with AlN nanoparticles by ultrasound-assisted stirring. *Mater. Sci. Eng. A* **2016**, *659*, 84–92. [[CrossRef](#)]
16. Sreekumar, V.M.; Babu, N.H.; Eskin, D.G. Prospects of In-Situ  $\alpha$ -Al<sub>2</sub>O<sub>3</sub> as an Inoculant in Aluminum: A Feasibility Study. *J. Mater. Eng. Perf.* **2017**, *26*, 4166–4176. [[CrossRef](#)]
17. Malaki, M.; Tehrani, A.F.; Niroumand, B. Fatigue behavior of metal matrix nanocomposites. *Ceram. Int.* **2020**, *46*, 23326–23336. [[CrossRef](#)]
18. Zhang, X.; Li, S.; Pan, B.; Pan, D.; Liu, L.; Hou, X.; Chu, M.; Kondoh, K.; Zhao, M. Regulation of interface between carbon nanotubes-aluminum and its strengthening effect in CNTs reinforced aluminum matrix nanocomposites. *Carbon* **2019**, *155*, 686–696. [[CrossRef](#)]
19. Kudryashova, O.B.; Eskin, D.G.; Khrustalev, A.P.; Vorozhtsov, S.A. Ultrasonic effect on the penetration of the metallic melt into submicron particles and their agglomerates. *Russ. J. Non-Ferrous Metals* **2017**, *58*, 427–433. [[CrossRef](#)]
20. Zhang, F.; Jacobi, A.M. Aluminum surface wettability changes by pool boiling of nanofluids. *Colloids Surf. A Physicochem. Eng. Asp.* **2016**, *506*, 438–444. [[CrossRef](#)]

21. Orlova, T.S.; Latynina, T.A.; Murashkin, M.Y.; Chabanais, F.; Rigutti, L.; Lefebvre, W. Effects of Mg on strengthening mechanisms in ultrafine-grained Al–Mg–Zr alloy. *J. Alloy. Compd.* **2021**, *859*, 157775. [[CrossRef](#)]
22. Zhang, H.M.; Zha, M.; Jia, H.L.; Tian, T.; Zhang, X.H.; Wang, C.; Ma, P.K.; Gao, D.; Wang, H.Y. Influences of the Al<sub>3</sub>Sc particle content on the evolution of bimodal grain structure and mechanical properties of Al–Mg–Sc alloys processed by hard-plate rolling. *Mater. Sci. Eng. A* **2021**, *802*, 140451. [[CrossRef](#)]
23. Fang, H.; Liu, H.; Yan, Y.; Luo, X.; Xu, X.; Chu, X.; Lu, Y.; Yu, K.; Wang, D. Evolution of texture, microstructure, tensile strength and corrosion properties of annealed Al–Mg–Sc–Zr alloys. *Mater. Sci. Eng. A* **2021**, *804*, 140682. [[CrossRef](#)]
24. Krishnan, B.P.; Surappa, M.K.; Rohatgi, P.K. The UPAL process: A direct method of preparing cast aluminium alloy-graphite particle composites. *J. Mater. Sci.* **1981**, *16*, 1209–1216. [[CrossRef](#)]
25. Javdani, A.; Pouyafar, V.; Ameli, A.; Volinsky, A.A. Blended powder semisolid forming of Al7075/Al<sub>2</sub>O<sub>3</sub> composites: Investigation of microstructure and mechanical properties. *Mater. Des.* **2016**, *109*, 57–67. [[CrossRef](#)]
26. Cao, X.; Shi, Q.; Liu, D.; Feng, Z.; Liu, Q.; Chen, G. Fabrication of in situ carbon fiber/ aluminum composites via friction stir processing: Evaluation of microstructural, mechanical and tribological behaviors. *Compos. Part B Eng.* **2018**, *139*, 97–105. [[CrossRef](#)]
27. Singh, R.; Singh, R.; Dureja, J.S.; Farina, I.; Fabbrocino, F. Investigations for dimensional accuracy of Al alloy/Al-MMC developed by combining stir casting and ABS replica based investment casting. *Compos. Part B Eng.* **2017**, *115*, 203–208. [[CrossRef](#)]
28. Philofsky, E. Intermetallic formation in gold-aluminum systems. *Solid-State Electron.* **1970**, *13*, 1391–1394. [[CrossRef](#)]
29. Dixit, S.; Kashyap, S.; Kailas, S.V.; Chattopadhyay, K. Manufacturing of high strength aluminium composites reinforced with nano tungsten particles for electrical application and investigation on in-situ reaction during processing. *J. Alloy. Comp.* **2018**, *767*, 1072–1082. [[CrossRef](#)]
30. Mohanty, P.S.; Gruzleski, J.E. Mechanism of grain refinement in aluminium. *Acta Metall. Mater.* **1995**, *43*, 2001–2012. [[CrossRef](#)]
31. Crossley, F.A.; Mondolfo, L.F. Mechanism of grain refinement in aluminum alloys. *JOM* **1951**, *3*, 1143–1148. [[CrossRef](#)]
32. Zhang, H.; Feng, P.; Akhtar, F. Aluminium matrix tungsten aluminide and tungsten reinforced composites by solid-state diffusion mechanism. *Sci. Rep.* **2017**, *7*, 12391. [[CrossRef](#)] [[PubMed](#)]
33. Dercz, G.; Piątkowski, J. Rietveld quantitative and structural analysis of the Al–W master alloy for silumina modification. In *Solid State Phenomena*; Trans Tech Publications Ltd.: Freienbach, Switzerland, 2010; Volume 163, pp. 161–164.
34. Zhang, Z.; Chen, D.L. Contribution of Orowan strengthening effect in particulate-reinforced metal matrix nanocomposites. *Mater. Sci. Eng. A* **2008**, *483–484*, 148–152. [[CrossRef](#)]
35. Sreekumar, V.M.; Babu, N.H.; Eskin, D.G.; Fan, Z. Structure–property analysis of in-situ Al–MgAl<sub>2</sub>O<sub>4</sub> metal matrix composites synthesized using ultrasonic cavitation. *Mater. Sci. Eng. A* **2015**, *628*, 30–40. [[CrossRef](#)]
36. Ramakrishnan, N. An analytical study on strengthening of particulate reinforced metal matrix composites. *Acta Mater.* **1996**, *44*, 69–77. [[CrossRef](#)]
37. Promakhov, V.V.; Khmeleva, M.G.; Zhukov, I.A.; Platov, V.V.; Khrustalyov, A.P.; Vorozhtsov, A.B. Influence of Vibration Treatment and Modification of A356 Aluminum Alloy on Its Structure and Mechanical Properties. *Metals* **2019**, *9*, 87. [[CrossRef](#)]
38. Dieringa, H.; Katsarou, L.; Buzolin, R.; Szakács, G.; Horstmann, M.; Wolff, M.; Mendis, C.; Vorozhtsov, S.; StJohn, D. Ultrasound Assisted Casting of an AM60 Based Metal Matrix Nanocomposite, Its Properties, and Recyclability. *Metals* **2017**, *7*, 388. [[CrossRef](#)]
39. Belov, N.A. Effect of eutectic phases on the fracture behavior of high-strength castable aluminum alloys. *Met. Sci. Heat Treat.* **1995**, *37*, 237–242. [[CrossRef](#)]